


Design of a linear to circular polarization converter integrated into a concrete construction for radome applications

Murat Öztürk¹, Umur Korkut Sevim¹, Olcay Altıntaş² , Emin Ünal²,
Oğuzhan Akgöl², Muharrem Karaaslan² and Cumali Sabah^{3,4}

Research Paper

Cite this article: Öztürk M, Sevim UK, Altıntaş O, Ünal E, Akgöl O, Karaaslan M, Sabah C (2022). Design of a linear to circular polarization converter integrated into a concrete construction for radome applications. *International Journal of Microwave and Wireless Technologies* **14**, 824–831. <https://doi.org/10.1017/S175907872100101X>

Received: 23 February 2021
Revised: 9 June 2021
Accepted: 9 June 2021
First published online: 5 July 2021

Keywords:

Concrete; meta-concrete; metamaterial; polarization converter; radome

Author for correspondence:

Olcay Altıntaş,
E-mail: olcay.altintas@iste.edu.tr

¹Civil Engineering, Iskenderun Technical University, Iskenderun, Hatay, Turkey; ²Electrical and Electronics Engineering, Iskenderun Technical University, Iskenderun, Hatay, Turkey; ³Department of Electrical and Electronics Engineering, Middle East Technical University – Northern Cyprus Campus, Kalkanlı, Guzelyurt, TRNC/Mersin 10, Turkey and ⁴Kalkanlı Technology Valley (KALTEV), Middle East Technical University – Northern Cyprus Campus, Kalkanlı, Guzelyurt, TRNC/Mersin 10, Turkey

Abstract

In this paper, we present a linear to circular polarization converter integrated in a concrete structure to eliminate signal transmission problem originated from the concrete buildings in microwave regime. Two polarization converter samples and a control specimen made by traditional concrete are designed and their signal transmission responses are compared experimentally. Axial ratio values which can be calculated by the ratio between the co-polar transmission and cross-polar transmission results of the proposed samples are below 3 dB and highly sufficient for linear to circular polarization conversion activity. The operating frequency for the proposed sample 1 is between 6 and 6.5 GHz with 500 MHz of bandwidth. The proposed sample 2 exhibits dual-band operation covering frequency bands, 4.58–5.13 and 6.0–6.4 GHz with bandwidths of 550 and 400 MHz, respectively. Operating frequencies of the samples are in the WIMAX frequency bands. In addition, the linear to circular polarization converter design integrated to concrete has a huge potential to improve reflection and directivity parameters of many antennas if it is considered as a radome.

Introduction

Concrete is the most widely used construction material. It is a heterogeneous material which includes cement, aggregate, and water. As a result of reaction between cement and water, a plastic paste which holds filler aggregate together is produced. Concrete is brittle and resistant to compression stress but weak to tensile stresses naturally.

As concrete is the most used material in construction sector, there are numerous studies on different applications of this material in construction area. Demir and Keles studied radiation transmission behavior of concrete including boron. According to their study, boron addition in concrete is an effective way to limit radiation transmission through concrete [1]. Demir *et al.* studied radiation transmission behavior of low and high weight concretes which included colemanite. Their finding concludes that the linear attenuation coefficient decreases as the concentration of colemanite increases in the concrete [2].

Nowadays, linear to circular polarization conversion studies have gained a great importance as the linearly polarized wave badly affects many environmental situations such as bad weather conditions or Faraday rotation force in the ionosphere at lower frequencies [3, 4]. When the linearly polarized signal passed through a rainy or snowy weather medium, some issues such as reflectivity, phasing, multi-path, and absorption occur at the signal condition. Circularly polarized signal is more preferred as it is not affected badly by these abnormal conditions. Hence, the importance of the linear to circular polarization conversion studies increases dramatically in the last decade. Zhu *et al.* designed a linear to circular metasurface polarization converter at 2.45 GHz and they tested the performance of the structure by using two different patch antennas [5]. Cong *et al.* achieved a perfect broadband metamaterial polarization converter by manipulating electromagnetic wave at terahertz regime in a wideband configuration with tri-layer metasurfaces [6]. Chen *et al.* studied an ultra-wide band polarization converter having double-head arrow geometry in the microwave regime both numerically and experimentally [7]. Karkkainen and Stuchly presented a frequency-selective surface as a linear to circular polarization transformer which is also configurable for a narrow frequency band [8]. Doumanis *et al.* studied an anisotropic impedance surface as a low profile and broadband linear to circular polarization rotator. This study is achieved by determining reflection characteristics of the structure both numerically and experimentally [9]. Fonseca and Mangenot also studied electrically thin high-performance anisotropic impedance surface which provides dual-

Table 1. Physical properties of the fibers

	Length (mm)	Diameter (mm)	Tensile strength (N/mm ²)	Specific gravity	Young's modulus (N/mm ²)
Carbon steel fiber	60	0.75	1100	7.1	210 000

band linear to circular polarization conversion for broadband satellite applications [10]. Ranga *et al.* presented a frequency-selective surface transmission polarizer based on width modulated lines and slots between the frequencies of 25 and 40 GHz [11].

Besides these, many studies about metamaterials applied to concrete structures have been carried out by the researchers so far. Ozbey *et al.* improved wireless sensing system to measure displacement or strain in concrete members by employing a metamaterial-based structure [12]. Kim and Lee have used electromagnetic shielding of a concrete structure to obtain negative permittivity which is one of the metamaterial properties [13]. Ungureanu *et al.* achieved an auxetic-like metamaterial structure made by concrete to protect from the unpredicted seismic waves [14]. Nasrollahi *et al.* offered a non-destructive testing method for concretes by embedding metamaterial to the applied transducers [15]. Mitchell *et al.* proposed a metamaterial concrete slab called meta-concrete to manipulate electromagnetic and acoustic waves and absorb the energy of the shock waves [16].

The reinforced concretes which prevent signal transmission are also an issue to transmit a linearly polarized wave. Most of the power of the incident signal is reflected from the structures and this causes communication problems at GSM, WIFI, or WIMAX bands, etc. In this study, we propose a linear to circular polarization converter by examining the other studies in the literature to eliminate the transmission problems originated from the concrete structures. The proposed polarization converter is obtained from the carbon steel fibers placed in the concrete structure based on horizontal, vertical, and diagonal configuration. Two converter samples having different distances (1 and 2 cm) between the carbon steel fibers are prepared. A vector network analyzer (VNA) and two microwave horn antennas are used for the experimental study to observe the transmission response and axial ratio (AR) results. The results are obtained by comparing the control specimen made by self-concrete. The AR, which is the key parameter for linear to circular polarization studies, is calculated by dividing cross-polar transmission responses to co-polar ones. Thus, operating frequencies and AR bandwidths (ARBWs) of the proposed polarization converter samples are obtained by determining corresponding AR values below 3 dB. The proposed structures have sufficient polarization conversion activity at microwave frequency ranges and have huge potential to solve signal transmission issues which is a problem for the concrete constructions. The proposed study recommends the meta-concrete definition with a new perspective. This perspective gives the opportunity to use the meta-concrete as a polarization converter for future radome applications. In this respect, the meta-concrete studies will focus on novel microwave shields and cloaking devices based on fibers in concrete.

Mixture preparation

To prepare designed concrete mixture, Type I ordinary Portland cement, carbon steel fiber, coarse aggregate, fine aggregate, and water were used. Natural fine aggregate and coarse aggregate have nominal maximum size of 4 and 11 mm and they also

**Fig. 1.** Carbon steel fibers.

have fineness modulus of 2.65 and 5.30 and specific gravity of 2.58 and 2.61, respectively. Physical properties of the carbon steel fiber are listed in Table 1 and demonstrated in Fig. 1. For the concrete prepared, cement:water:aggregate and fine aggregate:coarse aggregate ratio was kept constant as 1:3:5 and 1, respectively.

Three different test groups were prepared. The first test specimen as a control sample was traditional concrete which includes cement, aggregate, and water with the explained proportions above. Mechanical and physical properties of the control sample are compressive strength, flexural tensile strength, and density of the control sample with 52 MPa, 5 MPa, and 2.4 g/cm³, respectively. The second and the third test specimens were prepared layer by layer with the inclusion of steel fibers placed between. A speed-controlled power-driven revolving pan mixer was used for mixing. Firstly, aggregate and cement were dry-mixed enough and water was then added to the dry mixture, the mixing was continued until reaching proper workability of the mixture. The mixture was then poured into 200 mm × 200 mm × 60 mm prisms. The schematic views of the designed concrete specimens are shown in Fig. 2. The control specimen does not include steel fiber, but the other two specimens have steel fibers with different fiber location and design which is demonstrated in Fig. 2 in detail. A day after molding, the specimens were demolded and cured in a water tank up to 28 days. After water cure, the specimens were air dried then EM tests were performed on the prepared specimens.

The aim of the study is transforming a linearly polarized signal into a circularly polarized signal by placing carbon steel fibers into the cement. The circular polarization conversion can be realized by providing a phase difference between transmitted signals. The circularly polarized signal includes two perpendicular components namely, vertical and horizontal electrical fields. One of them is the main component which is determined by the incident linearly polarized wave. The side component is originated from

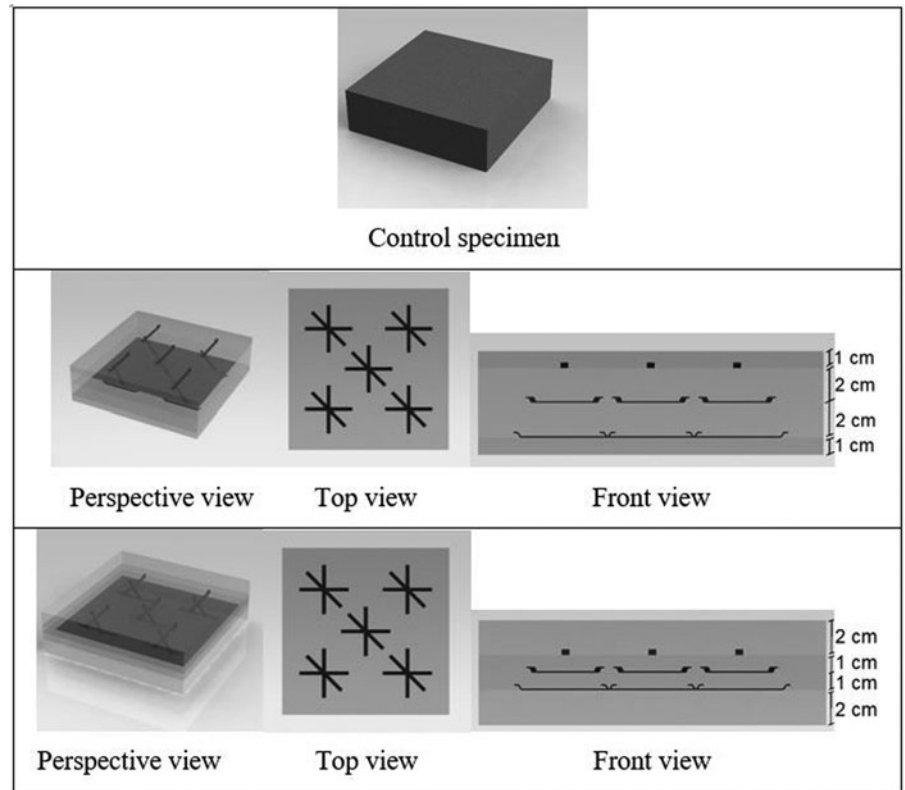


Fig. 2. The schematic views of the designed concrete specimens.

the main component by providing 90° phase difference. Hence, configurations of the carbon steel fibers as shown in Fig. 2 are implemented by horizontal, vertical, and diagonal lines to the obtained phase difference in transmitted signals.

Experimental results and discussion

The structure is proposed as a polarization rotator which converts linearly polarized signal to the circularly polarized one. The phenomenon can be validated by examining the AR of the circularly polarized signal. The AR(dB) can be described as;

$$\text{AR(dB)} = \text{Mag}(20 \log (\text{AR}(\omega)), \quad (1)$$

$$\text{AR}(\omega) = \frac{T(\omega)(\text{cross-polar})}{T(\omega)(\text{co-polar})}, \quad (2)$$

$$T(\omega) = |S_{12}|. \quad (3)$$

The experimental study is realized by Agilent PNA-L VNA having a range of 10 MHz to 43.5 GHz and two microwave horn antennas as illustrated in Fig. 3. The antennas were placed at a certain distance from the proposed structure to eliminate near field effect. Before the measurement, the VNA is calibrated by using free space measurement without the proposed structures. The structure is then placed between the horn antennas and co-polar and cross-polar transmission coefficients were measured. Co-polar response of the system is tested by the horn antennas having the same direction while the cross-polar responses are

measured by rotating one of the antennas 90°. Finally, the AR is calculated by dividing cross-polar response to co-polar response and it is converted into decibel (dB) through the formation referred in equation (1). The AR value should be below 3 dB for effective polarization conversion activity. In the same manner, operated frequency range or ARBW of the proposed polarization converter is determined by AR < 3 dB.

Co-polar and cross-polar transmission responses of the control specimen are shown in Fig. 4(a) with a frequency range of 5 GHz. This figure informs that the incident signal is not sufficiently transmitted through the control specimen between the frequencies of 3 and 8 GHz. In the same manner, AR does not occur at expected levels as shown in Fig. 4(b) due to insufficient cross-polar transmission value and the reflected signal from the structure is seen quite high. The purpose of the study is to observe and improve the transmission and AR values obtained from the control specimen as shown in Fig. 4. In accordance with this purpose, two different concrete samples are prepared by placing carbon steel fibers with different intervals and various combinations into the control specimen structure. The main reason for the selection of carbon fiber steel is to increase electrical interaction between incident wave and the proposed structure. Hence, the transmission level passed through the proposed structure will be increased by this carefully chosen material. In addition, the inclusion of carbon steel fibers in concrete provides a better resistance to tensile strengths by transferring excessive loads from weaker part to stronger part on the concrete.

First concrete sample which is created by placing the carbon fibers in the orientation of horizontal, vertical, and diagonal at 1 cm intervals was analyzed and the results are shown in Fig. 5. Transmission values for concrete samples are obtained by comparing the transmission magnitudes of the control specimen.

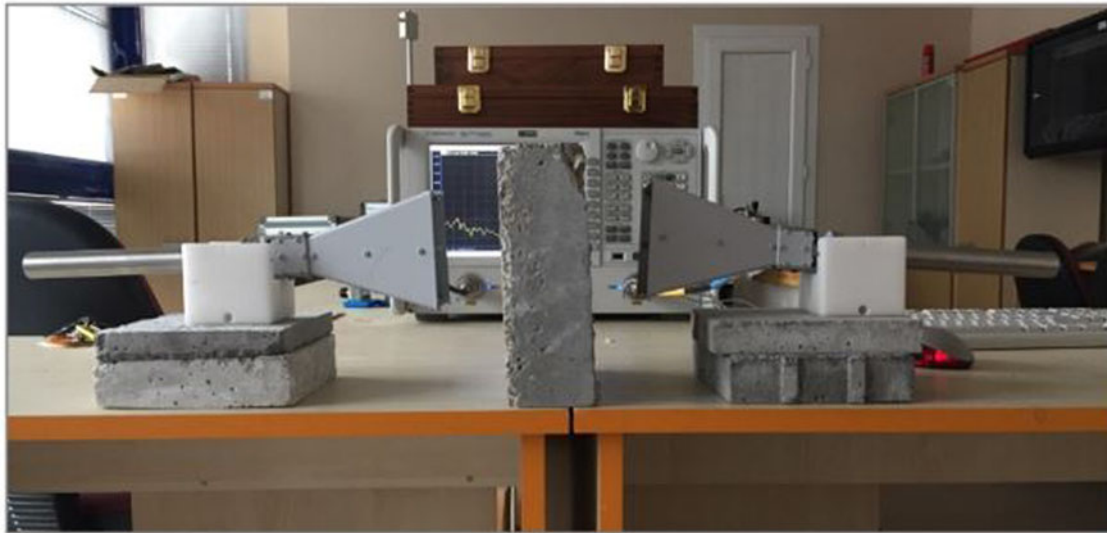


Fig. 3. Experimental setup.

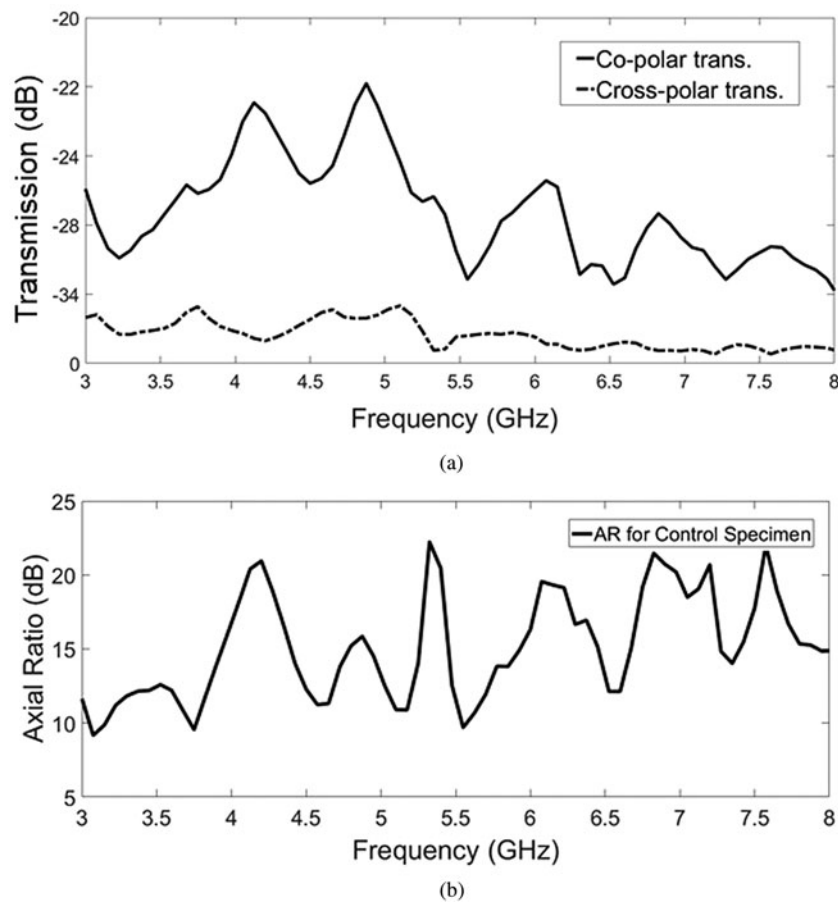


Fig. 4. (a) Co-polar and cross-polar transmission results and (b) the axial ratio for control specimen.

Sample 1 increased the co-polar transmission level about 5–10 times and cross-polar transmission level about 20–50 times with respect to control specimen between 3 and 8 GHz as shown in Fig. 5(a). Polarization conversion activity is successfully achieved by considering the AR result of the first sample plotted in Fig. 5 (b). The frequency range between 6 and 6.5 GHz can be accepted

as operating frequency range or namely ARBW of the proposed sample 1 since the AR is below 3 dB at this frequency band. Transmission magnitude values at this ARBW are equal to approximately 0.35 for both co-polar and cross-polar responses. When the transmission and reflection responses of control specimen are considered as given in Fig. 4, it can be easily said that the

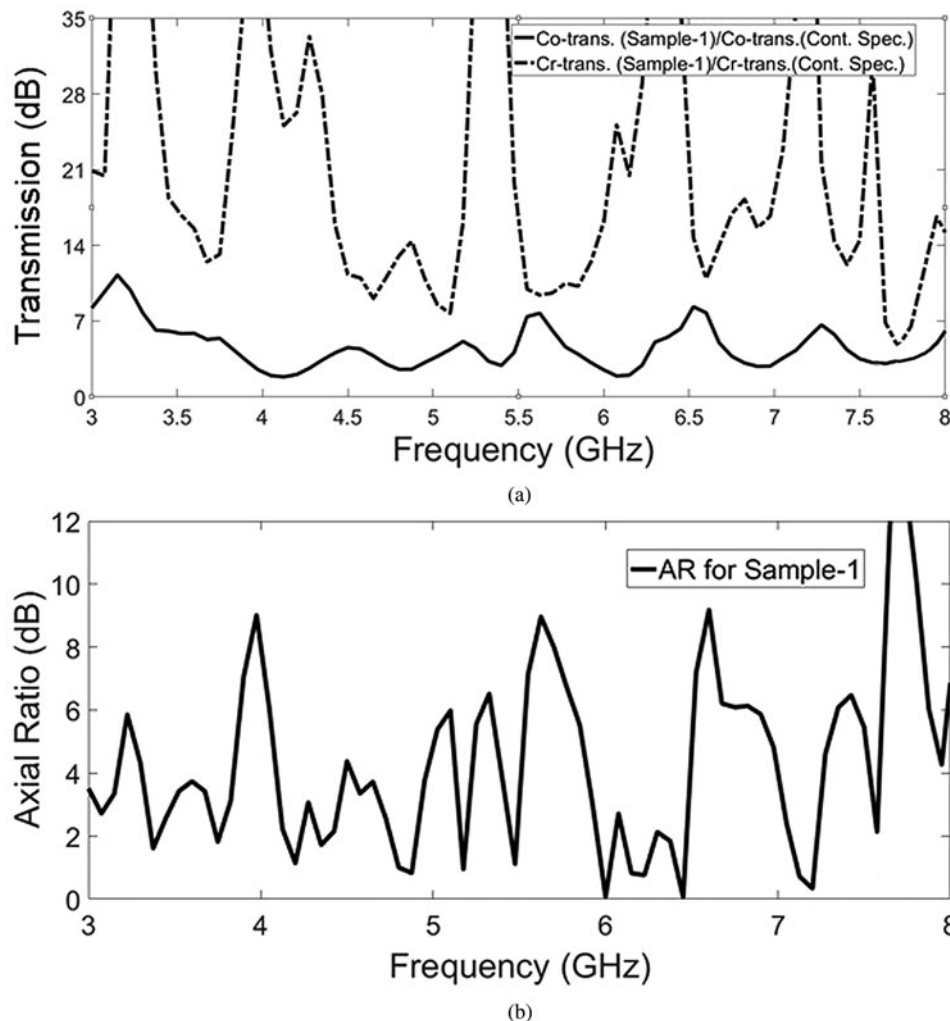


Fig. 5. (a) Co-polar and cross-polar transmission results and (b) the axial ratio for sample 1.

reflected signal from the concrete sample 1 was decreased and the transmitted signal was improved as shown in Fig. 5. Moreover, it can be concluded that the proposed polarization converter provides a circular polarization at many frequency bands including 4.08–4.42, 4.80–4.92, and 7.02–7.18 GHz which was represented in Fig. 5(b).

The reflection magnitude and phase level (degree) between the frequency range of 6 and 6.5 GHz are shown in Fig. 6. This frequency range is chosen due to high AR as mentioned above. The reflection magnitude is lower than 50% in all frequency ranges. Especially, the reflection coefficient is below 0.2 between 6 and 6.1 GHz. This reflection level is considerably low for a radome design. Besides this, the reflection phase is around 0° between 6.2 and 6.4 GHz. Hence, the reflected wave is in phase with the incident wave. As a result, the incident wave reduction will be in a low level.

The second proposed structure has the same configuration as the previous one having horizontal, vertical, and diagonal carbon steel fiber lines. Unlike the other design, the range between the lines in sample 2 is arranged as 2 cm. Co-polar, cross-polar transmission responses, and AR graph of the structure are illustrated in Fig. 7. Co-polar and cross-polar transmission levels plotted in Fig. 7(a) are 10–15 and 30–80 times stronger than control

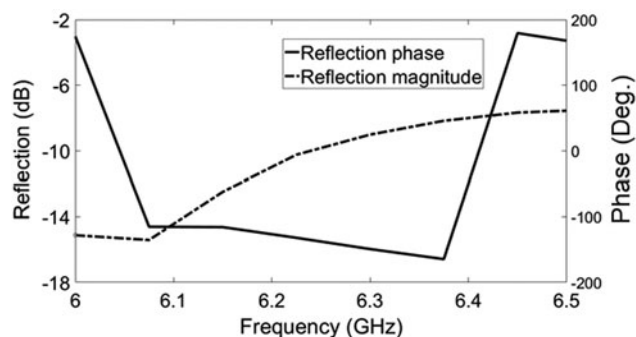


Fig. 6. Measured reflection phase and magnitude graph of the proposed sample 1.

specimen transmission responses, respectively. Therefore, the transmission magnitudes are observed at around 0.40 for both co-polar and cross-polar responses. The AR below 3 dB occurred in many frequency bands such as 3.32–3.76, 4.00–4.48, 4.58–5.13, 6.00–6.40, and 6.54–6.82 GHz as shown in Fig. 7(b). As the efficient polarization conversion occurs where the AR is near zero, operating frequency bands can be determined as 4.58–5.13 and 6.00–6.40 GHz. The ARBW's are about 550 and 400 MHz at

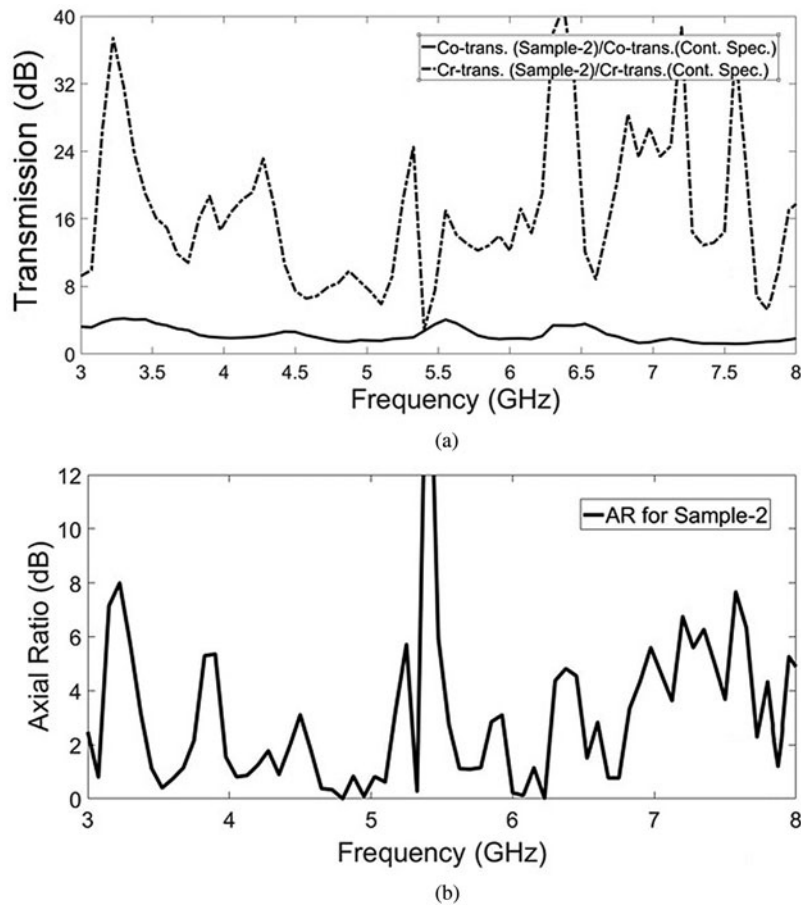


Fig. 7. (a) Co-polar and cross-polar transmission results and (b) the axial ratio for sample 2.

these bands. It can be concluded that the proposed sample 2 efficiently converts the incident linearly polarized signal into a circularly polarized signal at these two frequency bands. Moreover, it can also be said that sample 2 provides more efficient signal transmission and AR than the control specimen and sample 1 as shown in Fig. 7. The AR response of sample 2 is better than sample 1. The higher AR needs the conversion of the incident wave into transmitted wave with two components. One of the components has the same polarization (co-polar) and the other component must be rotated 90° (cross-polarized) with respect to the incident wave. Higher degree of cross-polarization and AR is provided by the second sample due to cross and close placement of the steel fiber which enhances the cross-polarization levels.

The magnitudes and phases of the reflection behavior of the proposed sample 2 between 4.58–5.13 and 6.00–6.40 GHz frequency bands are shown in Fig. 8. These frequency bands are chosen due to the significant ARs. The amplitude of reflection is lower than 0.6 and it reduces down to 0.2 at 4.9 GHz for the first band (4.5–5.3 GHz). The reflection is below 0.4 in the frequency range of 4.7–5.1 GHz. Hence, the proposed structure with high AR and relatively low reflection level can be applied in radome applications in this frequency range. The reflection phase is between 0 and 90 degrees in the first range. It means that the incident and reflected wave interact with each other. Since the phase difference is not around 180° , the attenuation of the incident wave due to reversely directed reflected wave will be in a limited level. Whereas the reflection magnitude is almost below 0.4, the phase of the reflected wave is around 180° in the second frequency band range. Therefore, the phase of sample 2

must be improved to reduce interaction between the incident and reflected waves.

The transmission and AR results for both sample 1 and sample 2 have been presented in Figs 9 and 10 to compare and better understand the operating frequency bands. The different distances between the carbon steel fibers for sample 1 and sample 2 (given in Table 2) cause different capacitive effects on the overall capacitance of the system. Hence, the resonance frequency and the transmission ratio have been affected by these capacitive variations as illustrated in Fig. 9. Moreover, it can be seen in Fig. 10 that sample 2 has a stronger AR result than sample 1 with respect to 0 dB at the frequency bandwidth between 6 and 6.40 GHz. This relation can be also seen at the other operating frequency bandwidth (between 4.58 and 5.13 GHz) of sample 2.

Conclusion

In this study, we present polarization rotator concrete samples which transform a linearly polarized incident wave into a circularly polarized wave at microwave frequency ranges. The ARs of the proposed concretes are obtained by dividing cross-polar transmission responses to co-polar ones. Their polarization conversion efficiencies are observed by comparing transmission values of a control specimen and by determining the ARBs below 3 dB. First concrete sample has 500 MHz ARBW between the frequencies of 6.00 and 6.50 GHz. The second one has two efficient operating frequencies between 4.58–5.13 and 6.00–6.40 GHz. It is concluded that the proposed structures can transform the linearly polarized wave into the circularly polarized one effectively

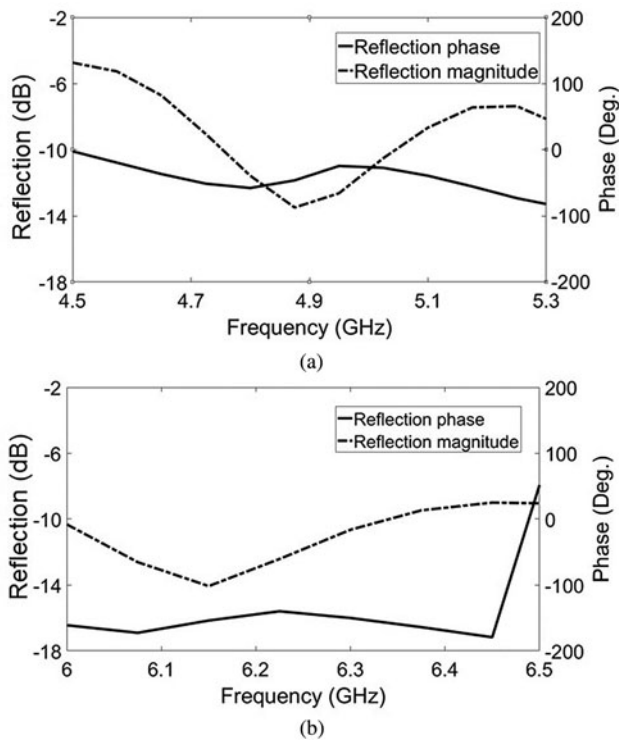


Fig. 8. Measured reflection phase and magnitude graph of the proposed sample 2 at operating frequency bands of (a) 4.58–5.13 GHz and (b) 6.00–6.40 GHz.

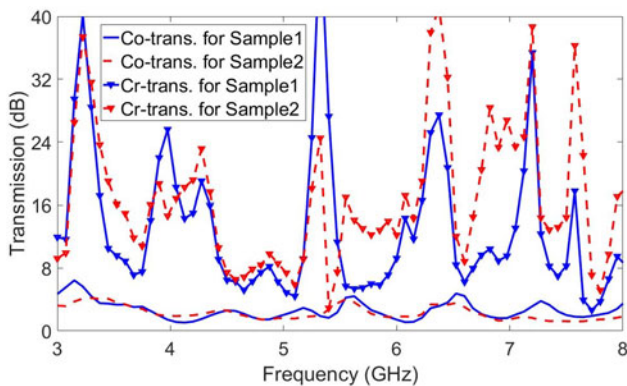


Fig. 9. Co-polar and cross-polar transmission results for both sample 1 and sample 2.

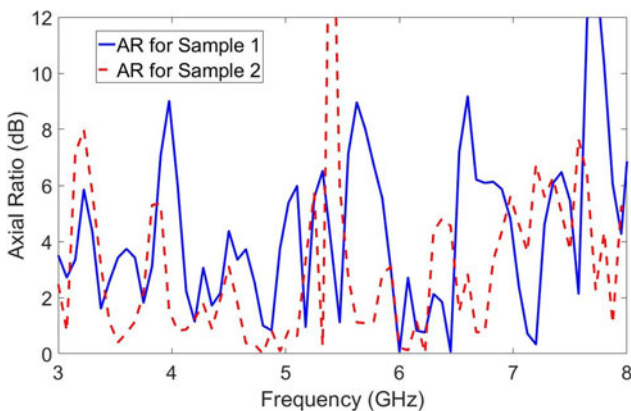


Fig. 10. Axial ratio results for both sample 1 and sample 2.

Table 2. Axial ratio, co-polar, and cross-polar transmission results for all samples

	Carbon steel fiber distance	Co-polar transmission	Cross-polar transmission	Axial ratio (<3 dB)
Control sample	–	–28 dB	–36 dB	–
Sample 1	1 cm	5–10 times of control sample	20–50 times of control sample	500 MHz
Sample 2	2 cm	10–15 times of control sample	30–80 times of control sample	950 MHz in total

considering the transmission ratios, reflection magnitude, and phase. Besides, the study shows that the operating frequency band of the structure can easily be adjusted to any desired frequency range such as WIFI or GSM band with simple adjustments. Moreover, the proposed polarization rotator is suitable for building constructions to transmit signals more efficiently and it can be integrated to the radomes of antennas to increase the efficiency. This study will be a myriad and it will change the meta-concrete definition. While meta-concrete studies in literature usually interest with mechanical properties of the designed structure, the proposed concrete with novel electromagnetic characteristics is a new type. The meta-concrete with a new perspective can provide high shielding for electromagnetic field security, huge values of AR for radome applications, and novel cloaking in buildings for both acoustic and microwave signals.

References

- Demir D and Keleş G (2006) Radiation transmission of concrete including boron waste for 59.54 and 80.99 keV gamma rays. *Nuclear Instruments and Methods in Physics Research Section B: Beam Interactions with Materials and Atoms* **245**, 501–504.
- Demir F, Budak G, Sahin R, Karabulut A, Oltulu M, Şerifoğlu K and Un A (2010) Radiation transmission of heavyweight and normal-weight concretes containing colemanite for 6MV and 18MV X-rays using linear accelerator. *Annals of Nuclear Energy* **37**, 339–344.
- Freeman A and Saatchi SS (2004) On the detection of Faraday rotation in linearly polarized L-band SAR backscatter signatures. *IEEE Transactions on Geoscience and Remote Sensing* **42**, 1607–1616.
- Lee KF and Luk KM (2011) *Microstrip Patch Antennas*. London: Imperial College Press.
- Zhu HL, Cheung SW, Chung KL and Yuk TI (2013) Linear-to-circular polarization conversion using metasurface. *IEEE Transactions on Antennas and Propagation* **61**, 4615–4623.
- Cong L, Cao W, Zhang X, Tian Z, Gu J, Singh R, Han J and Zhang W (2013) A perfect metamaterial polarization rotator. *Applied Physics Letters* **103**, 171107.
- Chen H, Wang J, Ma H, Qu S, Xu Z, Zhang A, Yan M and Li Y (2014) Ultra-wideband polarization conversion metasurfaces based on multiple plasmon resonances. *Journal of Applied Physics* **115**, 154504.
- Karkkainen K and Stuchly M (2002) Frequency selective surface as a polarisation transformer. *IEE Proceedings – Microwaves, Antennas and Propagation* **149**, 248–252.
- Doumanis E, Goussetis G, Tornero JLG, Cahill R and Fusco V (2012) Anisotropic impedance surfaces for linear to circular polarization conversion. *IEEE Transactions on Antennas and Propagation* **60**, 212–219.
- Fonseca NJG and Manganot C (2016) High-performance electrically thin dual-band polarizing reflective surface for broadband satellite applications. *IEEE Transactions on Antennas and Propagation* **64**, 640–649.

11. **Ranga Y, Thalakituna D, Esselle K, Hay SG, Matekovits L and Orefice M** (2013) A transmission polarizer based on width modulated line and slots, antenna technology (iWAT), Germany.
12. **Ozbey B, Erturk VB, Demir HV, Altintas A and Kurç Ö** (2016) A wireless passive sensing system for displacement/strain measurement in reinforced concrete members. *Sensors* **16**, 1–17.
13. **Ho-Yong K and Hong-Min L** (2010) *Application of Meta-material Concepts, in Microwave and Millimeter Wave Technologies from Photonic Bandgap Devices to Antenna and Applications*. InTech, pp. 103–132. doi:10.5772/212.
14. **Ungureanu B, Achaoui Y, Enoch S, Brule S and Guenneau S** (2015) Auxetic-like metamaterials as novel earthquake protections. arXiv preprint arXiv:1510.08785.
15. **Nasrollahi A, Deng W, Rizzo P, Vuotto A and Vandenbossche JM** (2017) Nondestructive testing of concrete using highly nonlinear solitary waves. *Nondestructive Testing and Evaluation* **32**(4), 381–399.
16. **Mitchell SJ, Pandolfi A and Ortiz M** (2016) Effect of brittle fracture in a metaconcrete slab under shock loading. *Journal of Engineering Mechanics* **142**(4), 04016010.



Murat Öztürk received the B.Sc. degree from Gaziantep University, Turkey, the M.Sc. and Ph.D. degree from Iskenderun Technical University, Turkey, all in Civil Engineering, in 2014, 2017, and 2021, respectively. He is currently working with Iskenderun Technical University, Hatay, Turkey. His research interests include EMI shielding, concrete, and smart materials.



Umur Korkut Sevim received the Ph.D. degree in Civil Engineering Department from the University of Cukurova, Adana, Turkey, in 2003. He is currently working with Iskenderun Technical University, Hatay, Turkey. His research interests are concrete, construction materials, and concrete admixture.



microwave regime.

Olcay Altıntaş received a Ph.D. degree in Electrical and Electronics Engineering at Cukurova University in 2020. He is the author of over 30 scientific papers published in SCI/SCI Expanded journals. He is currently working at Iskenderun Technical University as a researcher. His main research interests include metamaterial-based sensors, absorbers, energy harvesters, and polarization converters in the



Emin Ünal received his Ph.D. degree in Electrical and Electronics Engineering from the University of Gaziantep, Turkey, in 1994. He has authored more than 150 research articles and conference proceedings. His research interest includes analysis and synthesis of antennas, waveguides, FSS, and metamaterials.



Oğuzhan Akgöl received the B.Sc., M.Sc., and Ph.D. degrees in Electrical and Electronics Engineering from the Inonu University, Turkey, Polytechnic University, Brooklyn, NY, USA; the University of Illinois at Chicago (UIC), Chicago, IL, USA. He is currently working in the Iskenderun Technical University, Hatay, Turkey. His research interests are EM scattering, antennas, and metamaterials.



Muharrem Karaaslan received the Ph.D. degree in Physics Department from the University of Cukurova, Adana, Turkey, in 2009. He has authored more than 100 research papers and conference proceedings. His research interests are applications of metamaterials, analysis and synthesis of antennas, and waveguides.



Cumali Sabah received the B.Sc., M.Sc., and Ph.D. degrees in Electrical and Electronics Engineering. He is currently Professor in the Electrical and Electronics Engineering Department at Middle East Technical University – Northern Cyprus Campus, where he is also Secretary General and Advisor to the President. His research interests include the microwave and electromagnetic investigation of unconventional materials and structures, wave propagation, scattering, complex media, metamaterials and their applications, and solar photovoltaic systems and applications.